In-situ Energy-Dispersive X-ray Diffraction Studies of Crystal Growth and Compound Conversion Under Solvothermal Conditions

Lars Engelke,*[a] Michael Schaefer,[a] Felix Porsch,[b] and Wolfgang Bensch[a]

Keywords: X-ray diffraction / Cell design / Kinetics / Solvothermal synthesis / Thioantimonates

The results of in-situ energy-dispersive X-ray diffraction under solvothermal conditions performed on isostructural, layered thioantimonates $Mn_2Sb_2S_5$·L (L = amine) demonstrate the great potential of the method. When the synthesis was carried out at low temperatures with L being 1,3-diaminopropane (DAP), two crystalline intermediate phases were detected which then grew and disappeared when product growth started. Surprisingly, when *N*-methyl-1,3-diaminopropane (MDAP) was used, no crystalline intermediates could be detected and the induction time was significantly shorter than for DAP. For reactions up to 100 °C and for higher temperatures with $\alpha < 0.8$ (α is the extent of reaction), the crystallisation is predominantly controlled by nucleation. Further progress of crystallisation ($\alpha > 0.8$) leads to a change of the dominant process and a diffusion-controlled mechanism is observed. During the reaction with diethylenetriamine (DIEN), three crystalline intermediates were detected prior to product growth. The induction time is longer than for the other two compounds. The crystallisation seems to be diffusion-controlled and is faster than for the DAP and MDAP compounds. In a solution of DIEN, the crystalline phases $Mn_2Sb_2S_5$·L (L = DAP or MDAP) are transformed into the DIEN product under solvothermal conditions, and a rigorous analysis of the intensities of the reflections suggests a partial dissolution of the crystalline starting materials followed by crystallisation of the DIEN material.

Introduction

The synthesis of new and exciting porous materials is directly related to the application of solvo- and hydrothermal techniques. Under these conditions, primary building units like the TO_4 tetrahedra used to prepare zeolites, and organic molecules, which can act as structure-directing agents, are often stable. The final products are formed from these units and/or molecules by heterogeneous multicomponent reactions. Hydrothermal methods are widely applied in the preparation of open framework lattices such as zeolites, zeotypes, and metal-substituted zeolites.[1−4] Such porous materials are of great interest because of their use in a range of molecular recognition applications, as catalysts, absorption materials, and for ion-exchange reactions.[5−7] Due to the large technological potential of porous materials, most experiments are devoted to the preparation of new compounds with new and unprecedented properties. In order to understand solvothermal reactions and their mechanisms and to allow systematic developments of these materials, however, kinetic analyses by in-situ methods are necessary. Since the first study of a zeolite with in-situ energy-dispersive X-ray diffraction using synchrotron radiation (EDXRD) in 1992,[8] several reports of the results of such in-situ experiments have been published[5,9−15] (see also citations in ref.[11]). The in-situ powder diffraction method, as well as the latest developments in the technology required for such challenging experiments, was reviewed very recently by Walton and O'Hare.[16] The direct observation of crystallisation offers several advantages over conventional ex-situ techniques like angular-dispersive X-ray diffraction (ADXRD) and the advantages of in-situ methods are well documented in the literature.[5,11,16] Most of the experiments were performed on oxides and only a few studies were done on sulfides, i.e. on the compounds $(Me_4N)_2Sn_3S_7$·H_2O,[12,17] $(C_7H_{13}N)Mn_{0.25}Ge_{1.75}S_4$·$H_2O$,[18] and $Mn_2Sb_2S_5$·DAP.[19]

It must be kept in mind that the syntheses of chalcogenides or oxide phases under solvothermal conditions are multi-component heterogeneous reactions between liquid and solid components, and the chief difficulty of these reactions is the very large number of possible reaction variables. Changing one of these variables affects the pathway and kinetics of the reactions in ways which are not well understood. A systematic exploration of the effect on the synthesis of changing each variable can be a very time-consuming and inefficient process. In-situ EDXRD is a powerful method that allows the study of crystallisation kinetics under real-time conditions and the effect of altering one variable on crystallisation and product formation can be monitored easily. Furthermore, the occurrence and decay of

[a] Institut für Anorganische Chemie, Universität Kiel,
Otto-Hahn-Platz 6/7, 24098 Kiel, Germany
Fax: (internat.) + 49-431/880-1520
[b] Mineralogisch-Petrologisches Institut, Universität Bonn,
Poppelsdorfer Schloß, 53115 Bonn, Germany
Fax: (internat.) + 49-40/8998-4475

crystalline intermediate phases can be detected and monitored.

During the last few years we have prepared several new chalcogenides under solvothermal conditions.[20−29] The layered thioantimonates(III) $Mn_2Sb_2S_5$·L[20−22] [L = 1,3-diaminopropane (DAP), *N*-methyl-1,3-diaminopropane (MDAP), and diethylenetriamine (DIEN)] are of special interest because they are isostructural and can be prepared in the laboratory as phase-pure products under very similar reaction conditions. Therefore, the Mn−Sb−S−L systems are suitable for the study of the crystallisation kinetics as a function of the amine. The results of conversion experiments should give hints about the kinetic and thermodynamic stability of the different compounds.

In the present contribution we report the results of experiments carried out on the compounds $Mn_2Sb_2S_5$·MDAP and $Mn_2Sb_2S_5$·DIEN. In addition, the results of in-situ studies concerning the stability of the crystalline thioantimonates as well as their conversion are presented.

Results and Discussion

It is well documented that under solvothermal conditions several experimental variables strongly influence the product formation,[12,13,31−33] one of the most critical parameters being the reaction temperature. Bearing in mind that solvothermal crystallisation is a multicomponent heterogeneous reaction, it is clear that changing one parameter will influence other parameters in a way which is not well understood.

Prior to the in-situ EDXRD investigations, it was necessary to conduct the syntheses of $Mn_2Sb_2S_5$·L under dynamic conditions, i.e. stirring the mixtures during the reaction. Ex-situ experiments were performed to determine the stability of the crystalline thioantimonates in basic amine solutions. Interestingly, when diethylenetriamine (DIEN) was added to crystalline $Mn_2Sb_2S_5$·L (L = DAP or MDAP) phase-pure $Mn_2Sb_2S_5$·DIEN was always formed. These results obtained with the ex-situ experiments encouraged us to study the transformation of the crystalline starting materials with the in-situ EDXRD technique.

Studies of the Mn−Sb−S−DAP System

Very recently we reported the results of in-situ EDXRD experiments performed on the system Mn, Sb, S with DAP as amine.[19] The most important results of the experiments can be summarised as follows: The induction time t_0 depends strongly on the reaction temperature and increases from 15 min at 130 °C to about 60 min at 105 °C. The product growth is significantly accelerated at higher temperature. Analysis of the crystallisation kinetics showed that similar effects occur between 105 and 125 °C. The best agreement is obtained with a first-order reaction and/or a phase-boundary-controlled mechanism. With increasing α (α is the extent of reaction) the mechanism changes suggesting consecutive kinetics as the reaction proceeds. At 130 °C and α > 0.75 a three-dimensional, diffusion-controlled process dominates.

One of the surprising results was the observation of a crystalline precursor and a crystalline intermediate phase at reaction temperatures below 105 °C (Figure 1). The preliminary analysis provided evidence for a close correlation between the composition and structure of the intermediate and final products.[19] To trap the precursor and the intermediate, several experiments with different mixtures were conducted to isolate and characterise the two unknown crystalline phases. When a mixture of Mn, S, and DAP was heated to the desired temperature the first unknown phase formed; subsequent addition of antimony led to the product formation. Obviously, the precursor is an antimony-free phase composed of Mn, S, and DAP. Unfortunately, it was not possible to index the diffraction pattern of this precursor, but EDS and elemental analyses yielded an Mn/S/DAP ratio of 2:5:2. The second crystalline intermediate contains Sb, but its nature is still not clear. All attempts to quench the phase failed and it must be concluded that it is converted or destroyed during the cooling procedure and the workup of the mixture. Such a decomposition of a compound which is stable under the synthetic conditions is not surprising and similar observations have been made by other groups who have studied oxide systems by in-situ EDXRD.[13−16]

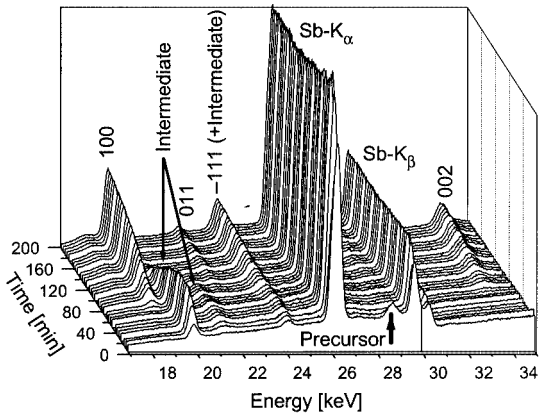

Figure 1. Time-resolved diffraction pattern of $Mn_2Sb_2S_5$·DAP recorded at 105 °C; the most prominent reflections of the two crystalline intermediates are marked; the numbers are reflection indices of the product

In-situ EDXRD Investigations of the Mn−Sb−S−MDAP and Mn−Sb−S−DIEN Systems

The experiments with MDAP and DIEN should show whether product formation with DAP, MDAP, and DIEN is identical or not. By comparing α with time for the three amines it is clear that product growth is significantly faster for MDAP than for DAP over the whole temperature range (see Figure 2). Between 85 and 120 °C the induction time t_0 is significantly shorter for MDAP (see Figure 3). The fastest growth was observed for DIEN but crystallisation needed the longest induction time. The DIEN reaction was therefore investigated in a temperature range from 110 to 170 °C.

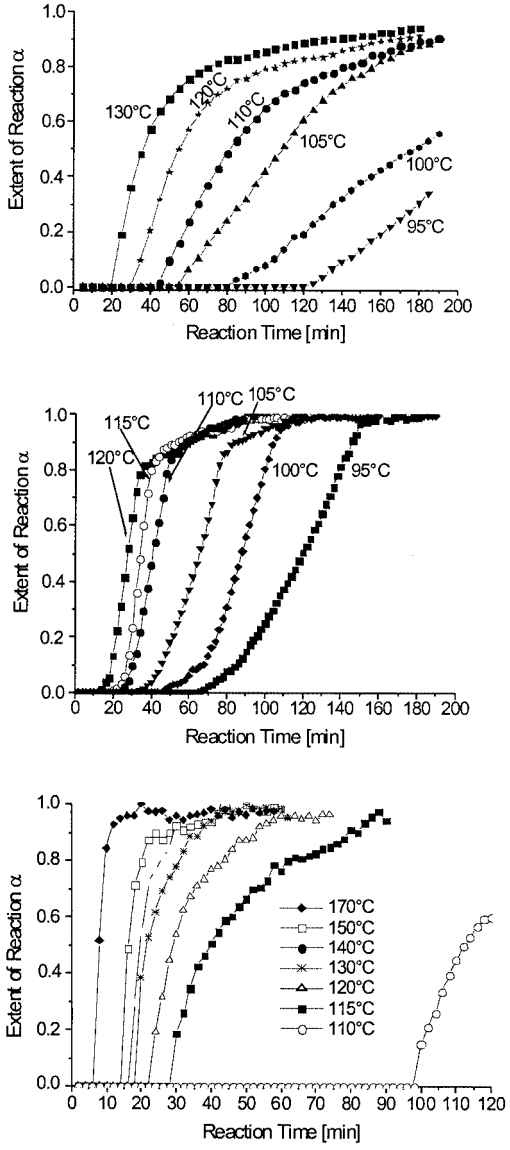

Figure 2. The extent of reaction (α) versus time for the (100) reflection of $Mn_2Sb_2S_5$·DAP (top), $Mn_2Sb_2S_5$·MDAP (centre) and $Mn_2Sb_2S_5$·DIEN (bottom) for different reaction temperatures

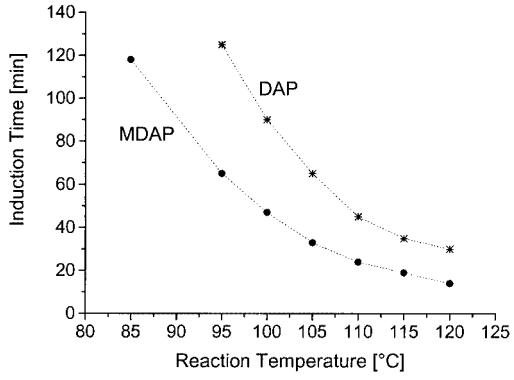

Figure 3. A comparison of the induction times t_0 for $Mn_2Sb_2S_5$·MDAP and $Mn_2Sb_2S_5$·DAP

In contrast to the experiments with DAP, no crystalline intermediate phases could be detected during the reaction with MDAP. All ex-situ and in-situ experiments to generate an analogue of the DAP precursor (see above) were unsuccessful. When using DIEN we observed a different pathway, as shown in Figure 4. First, an antimony-free precursor formed, as in the case of the DAP reaction. After a few minutes, the precursor disappeared, and this was followed by the occurrence of the first, short-lived, crystalline intermediate. A second crystalline compound was then seen which existed for a longer time. Finally, the product reflections of $Mn_2Sb_2S_5$·DIEN appeared.

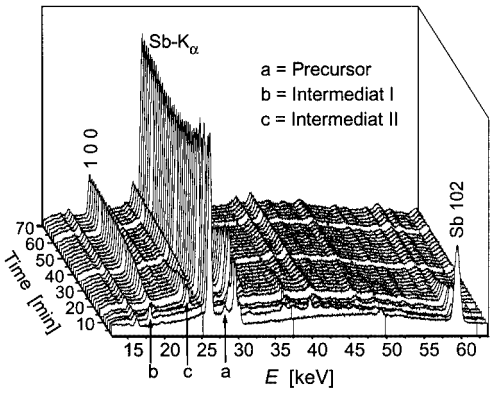

Figure 4. Time-resolved diffraction pattern of $Mn_2Sb_2S_5$·DIEN recorded at 130 °C; the most prominent reflections of the three crystalline intermediates are marked

These results suggest that in the early stages of the reactions, different consecutive and/or parallel mechanisms occur depending on the amine used. Analogous to the examinations of the DAP system,[19] kinetic studies were conducted with MDAP and DIEN. The spectra were collected every 120 s due to fast growth of the crystalline products. The intensity data were normalised with the Sb-K_α resonance and fitted to a theoretical expression relating α and time. The results were compared with expressions applied to solid-state kinetics. The general shapes of such expressions, represented graphically, are well documented.[13,34] The kinetic parameters were obtained by the Avrami−Erofeev expression $\alpha(t) = 1 - \exp[-(kt)^m]$ with α being the extent of reaction, m the reaction exponent and k [s^{-1}] the reaction rate coefficient.[35−37] The expression was then converted into the linear equation $\ln[-\ln(1-\alpha)] = m\cdot\ln(k) + m\cdot\ln(t)$ to analyse the product growth by a so-called Sharp−Hancock plot[34] plotting $\ln[-\ln(1-\alpha)]$ versus $\ln(t)$. Such a plot gives a straight line for that part of the reaction which follows the same mechanism. The reaction exponent m is obtained from the slope of the curve, whilst the rate constant k can be evaluated from the intercept with the y axis. The kinetic data obtained in this way for the MDAP reactions between 95 °C and 120 °C are listed in Table 1. For temperatures up to 100 °C a consistent mechanism was observed, being confirmed by the straight line through the points on the Sharp−Hancock plots (Figure 5, top). At higher temperatures two different regions can be

distinguished, with an inflexion point at $\alpha = 0.8$ (Figure 5, bottom). At $\alpha > 0.8$ a significantly lower reaction exponent m and a higher rate coefficient k were obtained. Due to the long induction times the DIEN data were collected between 110 and 170 °C (Table 2). After induction, the product growth is very fast. For larger α values the straight line in the Sharp−Hancock plots suggests a consistent mechanism.

Table 1. Kinetic data obtained by the analysis with Sharp−Hancock plots for crystallisation of $Mn_2Sb_2S_5$·MDAP; t_0 is the induction time, $t_{0.5}$ is the time when $\alpha = 0.5$

Reaction temp.	t_0 [s]	$t_{0.5}$ [s]	Rate constant k [s^{-1}]	Exponent (order) m
95 °C	3900	3300	$2.60(2)\cdot10^{-4}$	1.96(3)
100 °C	2800	2450	$3.69(7)\cdot10^{-4}$	3.13(6)
105 °C ($\alpha < 0.8$)	2000	1920	$4.40(6)\cdot10^{-4}$	1.97(3)
105 °C ($\alpha > 0.8$)			$7.01(8)\cdot10^{-4}$	1.07(6)
110 °C ($\alpha < 0.8$)	1350	1110	$7.75(5)\cdot10^{-4}$	2.27(4)
110 °C ($\alpha > 0.8$)			$1.36(9)\cdot10^{-3}$	0.78(6)
115 °C ($\alpha < 0.8$)	1100	970	$9.26(8)\cdot10^{-4}$	3.15(6)
115 °C ($\alpha > 0.8$)			$2.13(9)\cdot10^{-3}$	0.55(2)
120 °C ($\alpha < 0.8$)	800	850	$9.95(9)\cdot10^{-4}$	2.18(3)
120 °C ($\alpha > 0.8$)			$2.15(8)\cdot10^{-3}$	0.56(2)

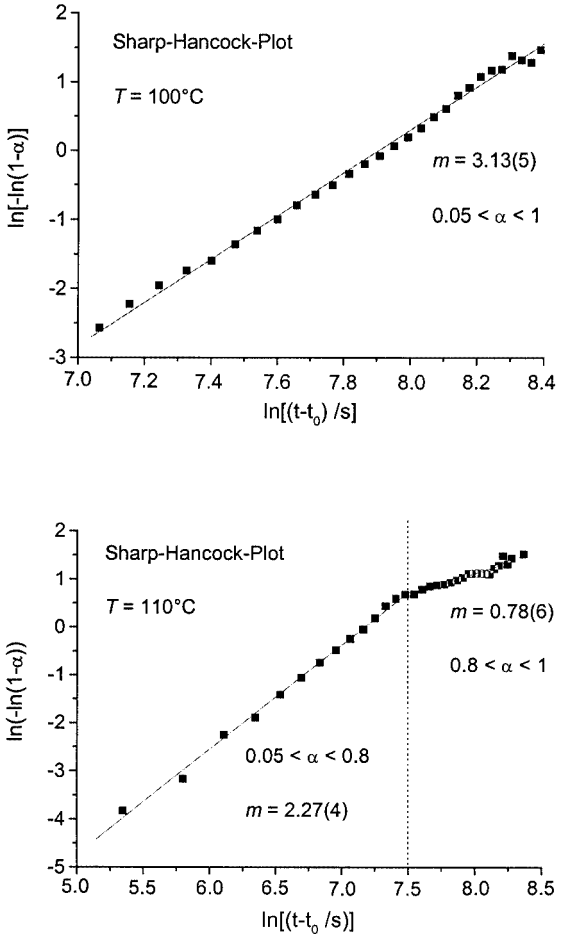

Figure 5. Sharp−Hancock plots of the data obtained for $Mn_2Sb_2S_5$·MDAP at 100 °C and 110 °C; experimental points are the solid squares and the lines represent the fits

Table 2. Kinetic data obtained by the analysis with Sharp−Hancock plots for the crystallisation of $Mn_2Sb_2S_5$·DIEN; t_0 is the induction time, $t_{0.5}$ is the time when $\alpha = 0.5$

Reaction temp.	t_0 [s]	$t_{0.5}$ [s]	Rate constant k [s^{-1}]	Exponent (order) m
110 °C ($\alpha < 0.6$)	5880	840	$7.64\cdot10^{-4}$	0.88(2)
110 °C ($\alpha > 0.6$)			$6.10\cdot10^{-4}$	0.44(2)
115 °C	1680	720	$8.86\cdot10^{-4}$	0.74(1)
120 °C	1320	440	$1.46\cdot10^{-3}$	0.87(2)
130 °C	1080	280	$2.79\cdot10^{-3}$	0.78(3)
140 °C	960	240	$5.38\cdot10^{-3}$	0.51(4)
150 °C	900	120	$7.84\cdot10^{-3}$	0.49(4)
160 °C	580	100	$8.87\cdot10^{-3}$	0.34(4)

To find a correct model for the crystallisation kinetics the data were plotted as $t/t_{0.5}$ versus α, with $t_{0.5}$ being the reaction time at $\alpha = 0.5$. Such a plot allows a direct comparison with the different models under consideration.[38] The different established models were compared with the experimental results (Table 3). For the temperatures up to 100 °C the $Mn_2Sb_2S_5$·MDAP crystallisation is predominately controlled by nucleation (Figure 6, top). This seems also to be the case for the reactions at higher temperatures with $\alpha < 0.8$. For the data with $\alpha > 0.8$ the curves are in reasonable agreement with a diffusion-controlled mechanism (D3) (Figure 6, bottom). It must be emphasised that such analyses are only approximations to the ideal borderline cases of the different models. Nevertheless, the data confirm that the crystallisation kinetics as well as the mechanisms are very different for the amines DAP and MDAP. The formation of $Mn_2Sb_2S_5$·DAP involves the formation and disappearance of two crystalline intermediates, and the crystallisation follows a phase-boundary-controlled mechanism. In contrast, for $Mn_2Sb_2S_5$·MDAP a nucleation-controlled growth without formation of any crystalline intermediate is observed. The proposed models are confirmed by the shapes of the α vs. time curves (Figure 2), which, as predicted by the theoretical models, are sigmoidal for nucleation-controlled mechanisms but not for phase-boundary-controlled models.[13] Interestingly, for the reaction with DIEN, different crystallisation kinetics are observed. Both, the shape of the curves and the $t/t_{0.5}$ data point to a diffusion-controlled mechanism. Due to the high rate constants the time resolution of 120 s is not adequate to determine low α values.

The activation energy of crystallisation was calculated by applying the Arrhenius equation $\ln(k) = \ln(A) - E_a/RT$. From the slope of an $\ln(k)$ versus $1/T$ plot, activation energies E_a of 65(5) kJ/mol (MDAP system) and 73(3) kJ/mol (DIEN system) were obtained. The values are in a range similar to those calculated for the crystallisation of the DAP compound as well as for usual zeolite compounds reported in the literature.[9,39] For the reactions with changing mechanisms the k values for $\alpha < 0.8$ were used.

Table 3. The rate equations for solid-state reactions reported in the literature

Growth model[38]	Rate equation f(α) = kt	m
Diffusion-controlled:		
$D_1(\alpha)$	$\alpha^2 = 0.25\ (t/t_{0.5})$	0.62
$D_2(\alpha)$	$(1-\alpha)\ln(1-\alpha)+\alpha = 0.1534\ (t/t_{0.5})$	0.57
$D_3(\alpha)$ [Jander]	$[1-(1-\alpha)^{1/3}]^2 = 0.0425\ (t/t_{0.5})$	0.54
$D_4(\alpha)$ [Ginstling−Brounshtein]	$1-2\alpha/3-(1-\alpha)^{2/3} = 0.0367\ (t/t_{0.5})$	0.57
Phase-boundary-controlled:		
$R_2(\alpha)$	$1-(1-\alpha)^{1/2} = 0.2929\ (t/t_{0.5})$	1.11
$R_3(\alpha)$	$1-(1-\alpha)^{1/3} = 0.2063\ (t/t_{0.5})$	1.07
First order		
F1(α)	$[-\ln(1-\alpha)] = 0.6931\ (t/t_{0.5})$	1.00
Nucleation [Avrami−Erovéef]:		
A2(α)	$[-\ln(1-\alpha)]^{1/2} = 0.8326\ (t/t_{0.5})$	2.00
A3(α)	$[-\ln(1-\alpha)]^{1/3} = 0.885\ (t/t_{0.5})$	3.00

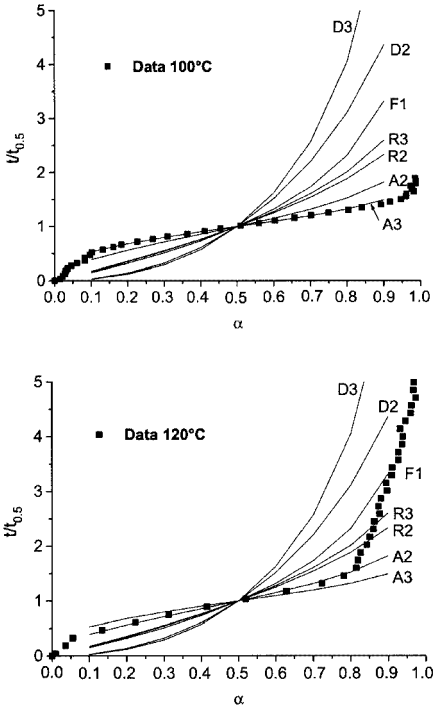

Figure 6. Comparison of the evolution of experimental $t/t_{0.5}$ data (T = 100 and 120 °C) as a function of α (black squares) with different kinetic models for $Mn_2Sb_2S_5$·MDAP; the letters with the numbers are the abbreviations of the different models listed in Table 2

Stability of Crystalline $Mn_2Sb_2S_5$·L Phases

In order to study the competition between the amines during product formation, 1:1 and 3:1 mixtures of two amines were examined and the reactions monitored. At the end of the reactions only one pure product containing only one amine was observed. The DAP/DIEN and MDAP/DIEN mixtures gave pure $Mn_2Sb_2S_5$·DIEN and for both mixtures the three crystalline phases were detected that were also seen using pure DIEN (see above). For DAP/MDAP mixtures the pure MDAP compound was formed, and even after 175 min no reflections of $Mn_2Sb_2S_5$·DAP were visible in the patterns. No hints were found for the appearance of the crystalline intermediate phases that were detected in the Mn−Sb−S−DAP system.

The conversion of the different isostructural phases which was observed with the ex-situ experiments was investigated in situ in the following way: The reactions with the amines DAP or MDAP, which gave the desired crystalline product, were monitored by in-situ EDXRD; after completion, 1 mL of a second amine was added to the product and spectra were recorded after 2 h at different temperatures to monitor possible changes in the starting material caused by the added amine.

After the addition of MDAP to the crystalline $Mn_2Sb_2S_5$·DAP product, no differences in the spectra could be detected even after 2 h at 120 °C (Figure 7). Very different results were obtained, however, when crystalline $Mn_2Sb_2S_5$·L (L = DAP or MDAP) products were treated with DIEN. The reaction between $Mn_2Sb_2S_5$·DAP and DIEN at 120 °C is relatively fast, and after about 45 min only reflections due to $Mn_2Sb_2S_5$·DIEN occurred in the pattern (Figure 8). The peak maximum of the (100) reflection shifts continuously from the position of $Mn_2Sb_2S_5$·DAP (18.74 keV) to that of $Mn_2Sb_2S_5$·DIEN (18.66 keV) as shown in Figure 9. The conversion of the DAP compound to the pure DIEN sample depends on the temperature, and the half-life was extended from about 10 min at 120 °C to 20 min at 110 °C.

Performing the experiments with crystalline $Mn_2Sb_2S_5$·MDAP resulted in the conversion into the DIEN product being slower. At 120 °C the appearance of reflections due to $Mn_2Sb_2S_5$·DIEN started after a few minutes but full conversion was not achieved for a further 2 h. Figure 10 shows the transformation of the MDAP to the DIEN phase. The temperature dependence is more pronounced than for DAP: The half-life has increased from 30 min at 120 °C to 120 min at 100 °C, and the completion requires several hours. These results suggest that $Mn_2Sb_2S_5$·DIEN is the most stable compound, followed by $Mn_2Sb_2S_5$·MDAP and $Mn_2Sb_2S_5$·DAP.

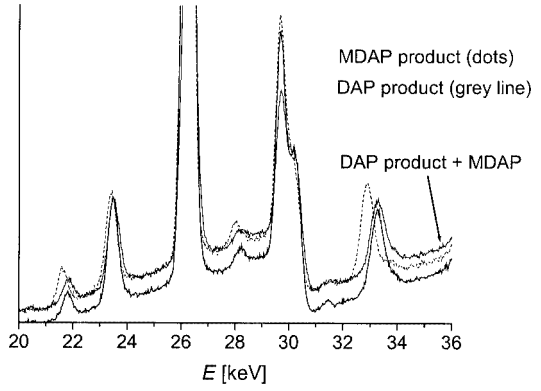

Figure 7. Comparison of the powder patterns of $Mn_2Sb_2S_5$·DAP and $Mn_2Sb_2S_5$·MDAP with the pattern measured after the reaction of $Mn_2Sb_2S_5$·DAP with a solution of MDAP

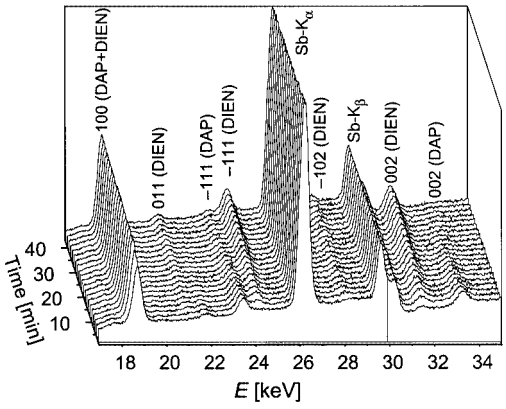

Figure 8. Time-resolved powder patterns collected during the conversion of $Mn_2Sb_2S_5$·DAP on adding DIEN at 120 °C; the indices of the reflections of the two phases are given

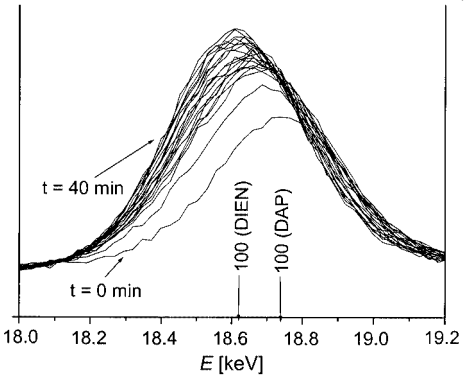

Figure 9. Subsequent shift of the position of the (100) reflection of $Mn_2Sb_2S_5$·DAP after DIEN addition

A quantitative evaluation of the change of MDAP into DIEN of the intensities of the (002) reflections at 100 and 120 °C is shown in Figure 11. Interestingly, the curves of the normalised intensities intersect at $\alpha \approx 0.5$ and several possibilities must be considered to explain this observation: i) direct solid-solid transformation, no amorphous intermediate, no dissolved phases involved in the process;

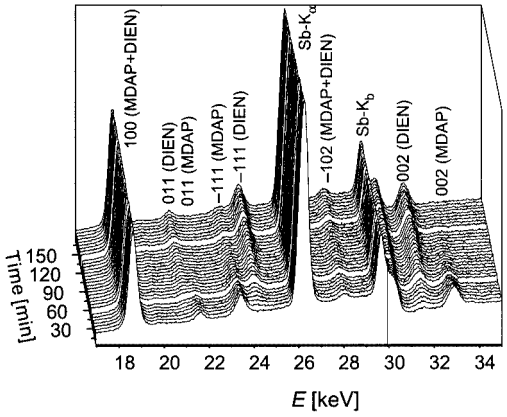

Figure 10. Time-resolved powder patterns collected during the conversion of $Mn_2Sb_2S_5$·MDAP applying DIEN at 120 °C; the indices of the reflections of the two phases are given

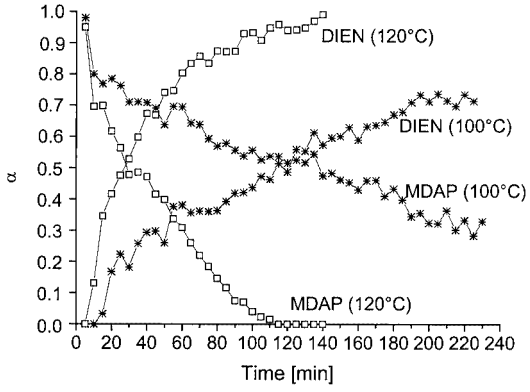

Figure 11. The evolution of the extent of reaction (α) for the (002) reflection of $Mn_2Sb_2S_5$·MDAP during the reaction with a DIEN solution monitored at 100 and 120 °C; note: the lines joining the symbols are only guides

ii) the first compound is completely converted into an amorphous phase, the product nucleates and crystallises subsequently;
iii) the first compound is completely dissolved and the product nucleates and crystallises from the solution;
iv) two completely separate processes for the formation of the first and the second product.

The decrease of the intensities of the DAP and MDAP compounds coincide with the occurrence of the reflections of the DIEN product. Therefore, explanation iv) can be immediately ruled out. Because the curves cross near $\alpha = 0.5$, a solid-solid transformation seems to be plausible, but partial dissolution or amorphisation of the starting material prior to crystallisation of the DIEN product cannot be excluded. A dissolution/amorphisation of a few percent of the DAP/MDAP starting material yields only minute changes in the intensities of the reflections.

It is highly likely that the transformation of the starting material compounds proceeds by one of the two mechanisms ii) or iii). To fully distinguish between these two possibilities other in-situ measurements are necessary. During

the syntheses of aluminophosphates intermediates were detected by in-situ NMR experiments. It is clear, however, that the Mn−Sb−S system is not suitable for such NMR investigations and other techniques such as in-situ Raman spectroscopy or in-situ XAS may provide the information necessary to understand what happens during the transformation of the intermediate into the final product. As demonstrated by Sankar[40,41] and Thomas[42] the combination of in-situ EDXRD and EXAFS is a powerful analytical tool for obtaining the missing information.

Conclusions

Despite the fact that $Mn_2Sb_2S_5$·DIEN, $Mn_2Sb_2S_5$·MDAP, and $Mn_2Sb_2S_5$·DAP are isostructural compounds, the mechanisms of formation are very different. For $Mn_2Sb_2S_5$·DAP crystallisation proceeds via two crystalline intermediates whereas for $Mn_2Sb_2S_5$·MDAP no hints for the formation of such intermediates were found. It is noteworthy that for the DIEN compound three crystalline precursors/intermediates could be detected. In addition, the data provide evidence that the crystallisation kinetics are different for the three compounds. For $Mn_2Sb_2S_5$·DAP, a first-order reaction or phase-boundary mechanism dominates at low temperatures, whereas at higher temperatures and $\alpha > 0.75$ a three-dimensional controlled process (D3) dominates. MDAP nucleation is the rate-limiting step in the low-temperature process and upon increasing the temperature the mechanism changes to D3 when $\alpha > 0.8$. Furthermore, the formation of $Mn_2Sb_2S_5$·MDAP requires shorter induction times than for the DAP analogue. The crystallisation of the DIEN compound proceeds by a diffusion-controlled mechanism after a significantly longer induction time.

The crystalline compounds $Mn_2Sb_2S_5$·DAP and $Mn_2Sb_2S_5$·MDAP are completely converted into the DIEN product suggesting that $Mn_2Sb_2S_5$·DIEN is the thermodynamically most stable compound of the isostructural samples. The difference in the stability between the DAP and MDAP compounds is too small for a transformation of DAP into MDAP. The rigorous analysis of the in-situ EDXRD data for the conversion of MDAP starting material into the DIEN product suggests that a small amount of $Mn_2Sb_2S_5$·MDAP is dissolved, followed by an immediate crystallisation of $Mn_2Sb_2S_5$·DIEN. It must be noted that the amount of the amine applied guarantees a 60-fold excess with respect to the elements Mn/Sb/S.

The results presented here clearly demonstrate that even for isostructural compounds the actual mechanism of formation is very different. Evidently, the amine used determines the mechanism of product crystallisation.

It is well documented that the reactions occurring in the heterogeneous mixture determine what type of compound nucleates and starts to crystallise. Because X-ray diffraction is "blind" with respect to the processes within the so-called induction period, future projects will focus on combined in-situ EXAFS/EDXRD experiments.

Experimental Section

The HASYLAB Beamline F3 receives white synchrotron radiation from a bending magnet with a critical energy of 16 keV and gives a positron beam energy of 4.5 GeV. An energy range from 13.5 to 65 keV can be observed with a maximum at about 20 keV. The diffracted beam is monitored by a nitrogen-cooled solid-state germanium detector. The detector angle was chosen so that all important Bragg reflections could be detected. The *d*-spacing range is given by $E = 6.199/(d \cdot \sin\theta)$. With a detector angle of approximately 1.96° the observable *d*-spacing range is 2.8 to 13.4 Å. Above 26 keV, the energy resolution $\Delta d/d$ is about 10^{-2}. The beam was collimated to 0.2 mm giving the best results.

The investigations were carried out in Teflon-lined autoclaves under autogenous pressure and isothermal conditions similar to those used for the ex-situ investigations in the laboratory. Because common steel autoclaves are not sufficiently permeable for synchrotron radiation, aluminium was used instead. Furthermore, the overall thickness of the wall of the autoclave was reduced from 2.5 mm to 1 mm. At the positions of beam inlet and outlet the wall thickness was machined down to 0.5 mm. The Teflon liner had an internal diameter of 10 mm, wall thickness of 1 mm, height of 94 mm and a capacity of 7 mL. A slightly different set-up for an in-situ cell was described by Evans et al.,[30] the smaller diameter should reduce absorption effects due to the pathway of the beam through the solution.

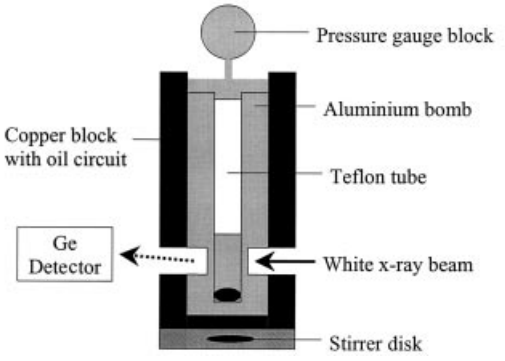

Figure 12. The experimental set-up used for the in-situ EDXRD experiments

The whole experimental set-up is shown in Figure 12 and the entire assembly was constructed according to the requirements of the desk of beamline F3 at HASYLAB in Hamburg. Time-resolved X-ray powder patterns with good counting statistics could be recorded with acquisition times of 300 s. A shorter acquisition time of 120 s was also used to obtain a higher resolution of induction times and reaction courses.

For the syntheses of $Mn_2Sb_2S_5$·L, elemental Mn (27.5 mg; 0.5 mmol), Sb (61.0 mg; 0.5 mmol), and S (40.0 mg; 1.25 mmol) were heated in a 70 % aqueous solution of the amines (2 mL) at temperatures ranging from 85 to 170 °C.

Acknowledgments

We gratefully acknowledge financial support from the State of Schleswig-Holstein, the Deutsche Forschungsgemeinschaft (DFG), and the Fonds der Chemischen Industrie (FCI).

[1] W. S. Sheldrick, M. Wachhold, *Angew. Chem. Int. Ed. Engl.* **1997**, *36*, 206−226.
[2] A. Rabenau, *Angew. Chem. Int. Ed. Engl.* **1985**, *24*, 1026−1040.
[3] M. T. Weller, S. E. Dann, *Curr. Op. Solid State Mater. Sci.* **1998**, *3*, 137−143.
[4] M. E. Davis, R. F. Lobo, *Chem. Mater.* **1992**, *4*, 756−768.
[5] J. M. Thomas, *Angew. Chem. Int. Ed.* **1999**, *38*, 3588−3628.
[6] R. Barrer, *Zeolites and Clay Minerals as Sorbents and Molecular Sieves*, Academic Press, London **1978**.
[7] H. van Bekkum, E. Flanigan, J. Jansen (Eds.), *Introduction to Zeolite Science and Practice*, Elsevier, Amsterdam **1991**.
[8] J. Munn, P. Barnes, D. Hausermann, S. A. Axon, J. Klinowski, *Phase Transitions* **1992**, *39*, 129−134.
[9] A. T. Davies, G. Sankar, C. R. Catlow, S. M. Clark, *J. Phys. Chem. B* **1997**, *101*, 10115−10120.
[10] P. Norby, J. C. Hanson, *Catal. Today* **1998**, *39*, 301−309.
[11] R. J. Francis, D. O'Hare, *J. Chem. Soc., Dalton Trans.* **1998**, 3133−3148.
[12] A. N. Christensen, T. R. Jensen, P. Norby, J. C. Hanson, *Chem. Mater.* **1998**, *10*, 1688−1693.
[13] R. J. Francis, S. O'Brien, A. M. Fogg, P. Halasyamani, D. O'Hare, T. Loiseau, G. Férey, *J. Am. Chem. Soc.* **1999**, *121*, 1002−1015.
[14] S. O'Brien, R. J. Francis, A. M. Fogg, D. O'Hare, N. Okazaki, K. Koruda, *Chem. Mater.* **1999**, *11*, 1822−1832.
[15] R. I. Walton, T. Loiseau, D. O'Hare, G. Férey, *Chem. Mater.* **1999**, *11*, 3201−3209.
[16] R. I. Walton, D. O'Hare, *Chem. Commun.* **2000**, 2283−2291.
[17] R. J. Francis, S. J. Price, J. S. O. Evans, S. O'Brien, D. O'Hare, *Chem. Mater.* **1996**, *8*, 2102−2108.
[18] C. L. Cahill, Y. Ko, J. C. Hanson, K. Tan, J. B. Parise, *Chem. Mater.* **1998**, 1453−1458.
[19] L. Engelke, M. Schaefer, M. Schur, W. Bensch, *Chem. Mater.* **2001**, *13*, 1383−1390.
[20] W. Bensch, M. Schur, *Eur. J. Solid State Inorg. Chem.* **1996**, *33*, 1149−1160.
[21] M. Schur, C. Näther, W. Bensch, *Z. Naturforsch., Teil B* **2001**, *56*, 79−84.
[22] L. Engelke, R. Stähler, M. Schur, C. Näther, W. Bensch, *Z. Anorg. Allg. Chem.*, in preparation.
[23] W. Bensch, M. Schur, *Z. Naturforsch., Teil B* **1997**, *52*, 405−409.
[24] W. Bensch, C. Näther, M. Schur, *Chem. Commun.* **1997**, 1773−1774.
[25] M. Schur, W. Bensch, *Eur. J. Solid State Inorg. Chem.* **1997**, *34*, 457−466.
[26] M. Schur, W. Bensch, *Z. Anorg. Allg. Chem.* **1998**, *624*, 310−314.
[27] F. Wendland, C. Näther, M. Schur, W. Bensch, *Acta Crystallogr., Sect. C* **1998**, *54*, 317−319.
[28] H. Rijnberk, C. Näther, M. Schur, I. Jeß, W. Bensch, *Acta Crystallogr., Sect. C* **1998**, *54*, 920−923.
[29] M. Schur, A. Gruhl, C. Näther, I. Jeß, W. Bensch, *Z. Naturforsch., Teil B* **1999**, *54*, 1524−1528.
[30] J. S. O. Evans, R. J. Francis, D. O'Hare, S. J. Price, S. M. Clark, J. Flaherty, J. Gordon, A. Nield, C. Tang, *Rev. Sci. Instrum.* **1995**, *66*, 2442−2445.
[31] A. M. Fogg, D. O'Hare, *Chem. Mater.* **1999**, *11*, 1771−1775.
[32] J. S. O. Evans, S. Price, H. Wong, D. O'Hare, *J. Am. Chem. Soc.* **1998**, *120*, 10837−10846.
[33] A. K. Cheetham, C. F. Mellot, *Chem. Mater.* **1997**, *9*, 2269−2279.
[34] J. D. Hancock, J. H. Sharp, *J. Am. Ceram. Soc.* **1972**, *55*, 74−76.
[35] M. Avrami, *J. Chem. Phys.* **1939**, *7*, 1103−1112.
[36] M. Avrami, *J. Chem. Phys.* **1940**, *8*, 212−224.
[37] M. Avrami, *J. Chem. Phys.* **1941**, *9*, 177−184.
[38] J. H. Sharp, G. W. Brindley, B. N. N. Achar, *J. Am. Ceram. Soc.* **1966**, *49*, 379−382.
[39] A. Gualtieri, P. Norby, G. Artoli, J. C. Hanson, *Phys. Chem. Miner.* **1997**, *24*, 191−199.
[40] G. Sankar, J. M. Thomas, F. Rey, G. N. Greaves, *J. Chem. Soc., Chem. Commun.* **1995**, 2549−2550.
[41] M. Epple, G. Sankar, J. M. Thomas, *Chem. Mater.* **1997**, *9*, 3127−3131.
[42] J. M. Thomas, *Chem. Eur. J.* **1997**, *3*, 1557−1562.

Received February 22, 2002
[I02089]